Available *online* at: http://journal.unj.ac.id

Jurnal Pensil | Pendidikan Teknik Sipil

Journal homepage: http://journal.unj.ac.id/unj/index.php/jpensil/index

ANALYSIS OF GLOBAL BEHAVIOUR AND STIFFNESS IN BOLTED CONNECTION FOR STEEL BEAM USING FINITE ELEMENT METHOD

Kritananda Tantra Halim[1], *Andy Prabowo*[2*], *Sunarjo Leman*[3]
[1,2] Program Studi Magister Teknik Sipil, Universitas Tarumanegara
Jl. Letjen S. Parman No. 1, Jakarta, 11440, Indonesia
[2] Program Studi Sarjana Teknik Sipil, Universitas Tarumanegara
Jl. Letjen S. Parman No. 1, Jakarta, 11440, Indonesia
Jl. Raya ITS, Keputih, Sukolilo, Surabaya, East Java 60111, Indonesia
[1]kritananda.education@gmail.com, [*2]sunarjo@ft.untar.ac.id, [3]andy.prabowo@ft.untar.ac.id

P-ISSN: 2301-8437
E-ISSN: 2623-1085

ARTICLE HISTORY
Accepted:
12 November 2025
Revision:
27 Januari 2026
Published:
31 Januari 2026

ARTICLE DOI:
10.21009/jpensil.v15i1.62014

Abstract

This research aims to analyse the differences in the properties and stress distribution of steel connections of the Splice Plate and End Plate types using finite element method. Connection are crucial structural element that influence the overall strength, stiffness and behaviour of steel structure, particularly in beam splices where failure modes under flexural and shear loads can vary significantly. The experiment was carried out to determine the more efficient connection type evaluat the stiffness variation based on connection location, and identify failure point under combined flexural and shear forces. The analysis was performed with literature review and testing using MIDAS FEA NX software with a non-linear approach on SS400 grade steel and A325 bolts. The connection design referred to SNI and AISC regulations, analyzing I-beam profiles (IWF) and both connection types. The modeling was performed at two positions: mid-span and beam edge (end-span). The analysis results showed a similar Load-Displacement curve pattern with a maximum load of approximately 200 kN before entering the plastic phase, leading to a deflection of 435–448 mm at the mid-span. Although both connections are nearly identical behavior, the Splice Plate connection demonstrated higher stiffness, while the End Plate connection seemed more efficient because it requires fewer bolts and less additional plating in the fabrication process.

Keywords: Steel Stress, Bolted Splice Connection, End Plate, Finite Element Method, FEM

Introduction

Connection are crucial in steel structures, as they can influence the overall strength, stiffness and behaviour of the structure (Dewobroto, 2015). Steel as a superior construction material possesses mechanical properties such as high strength, elasticity and ductility (Lesmana, 2021). However, weaknesses like corrosion, buckling and fatigur require special attention to connections (Arifi & Setyowulan, 2021). Bolted connection such as splice plate and end-plate are commonly used to join IWF beams, which primarily resist flexural and shear forces (Pertiwi et al., 2023). Abdi et al. (2017) highlight the importance of steel in construction, confirming the topic of steel as one of the crucial component mandatory in building material science course.

Previous studies have highlighted the behaviour of splice and end-plate connection. Tao et al. (2017) analyzed bolted end-plate connection to concrete-filled steel columns, demonstrating semi-rigid behaviour with significant rotational capacity under monotonic loading. Fakih et al. (2018) and Osman & Mourad (2021) investigated extended end-plate joints under static and dynamic loads, emphasizing deformation patterns and shear forces distribution in the bolt zones. For splices plate connections, He et al. (2020) conducted experimental tes ton prefabricated steel beams, noting high stiffness but vulnerabulity to block shear failure. Numerical models by Luo et al. (2020) and Song et al. (2024) optimized splice joints using FEM, focusing on bolt configurations and plate length to reduce strss concentrations.

Nevertheless, these studies have limitations, such as a primary focus on cyclic or seismic loading without comprehensive comparison between splice and end-plate type across mid-span and side plan positions (Bahaz et al., 2018; Diaz et al., 2018). Few researchers integrate SS400 steel with A325 bolts under combined flexural-shear condition per SNI/AISC standards, and there is a lack of nonlinear FEM studies emphasizing global behaviour up to failure.

This study addresses these gaps by comparatively evaluating splice and end-plate connections in varying positions using nonlinear FEM in MIDAS FEA NX, with a focus on stiffness, load capacity and failure modes. The novelty lies in benchmarking against plain IWF beams to assess practical efficiency in seismic prone region like Indonesia, potentially reducing fabrication costs and material waste. This research aims to analyze the difference in mechanical properties and stress distribution of splice plate and end-plate steel connections compared to a plain IWF beamu sing the nonlinear finite element method on SS400 steel and A325 bolts, with variations in connection positions at mid-span and side-span up yo failure.

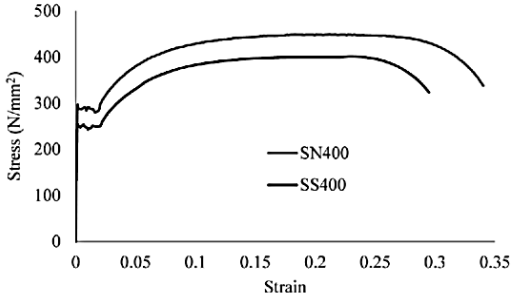

Figure 1. Graph Stress Strain Steel SS400 and SN400 (Yamada & Jiao, 2016)

Finite Element Method (FEM) analysis on SS400 material was previously conducted by *Hai et al. (2020)*. This experiment focused on a 6 mm thick SS400 steel plate subjected to pressure until it formed a V-shape. Their study also compared the results obtained from the experimental work with those from the FEM simulation. Research investigating the behaviour of IWF (Wide Flange) steel beams with SS400 grade using an effective hysteretic model successfully stimulated the mechanical behaviour of the beams. The results of this cyclic hysteretic study showed a decomposition into skeleton curves and Bauschinger parts *(Yamada & Jiao, 2016)*.

Table 1. Chemical Property and Composition of JISG3101 – SS400

C	Si	Mn	P	S	Cr	Fy (MPa)	Fu (MPa)
0.19-0.21	0.05-0.17	0.4-0.6	0.04	0.5	< 0.3	215-245	400-550

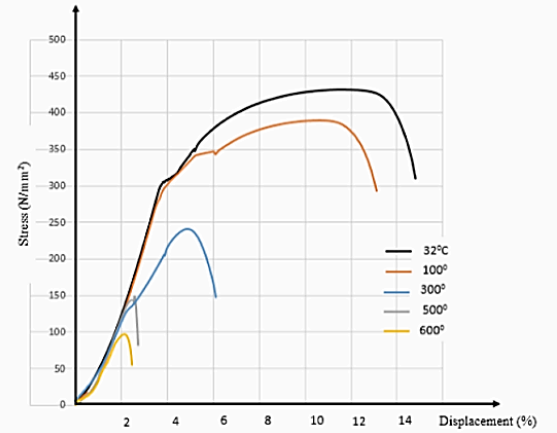

Figure 2. Graph Curve Stress-Displacement SS400 on High Temperature
(Vuong et al., 2019)

A beam is a flexural structure that resists gravity loads, dead loads, live loads, and combined lateral loads (earthquake). The beam structural component is a combination of compression and tension elements. A beam is a structural element that spans horizontally and is primarily loaded vertically (Pertiwi et al., 2023). Beam-column connections are joints whose behavior significantly influences the overall structural system. The resulting connection behavior lies between a rigid connection and a simple connection, referred to as a semi-rigid or partially restrained (PR) connection (Tayu et al., 2017).

Flexural elements function primarily to resist internal forces caused by external loads, predominantly in the form of bending moments. In steel structure design, IWF sections are commonly used because they offer a relatively high economic value compared to other profile types (Arifi & Setyowulan, 2021). The joining process in the fabrication workshop is carried out using precise tools and is easily supervised to ensure controlled quality. These structural elements are then transported to the field to be assembled according to the plan. The two common types of connections used are bolted and welded connections (ACI Committee 318, 2014).

In the execution of steel connections, a specific connection system must be used, which depends on the type of elements being joined and the situation. The connection system for IWF steel components will differ from that used for a Cremona truss. Therefore, determining the type of connection is crucial for the chosen structural analysis and affects the distribution of forces in the connection area (Pertiwi et al., 2023). Correct structural components support the achievement of safe and sustainable building design (Linggasari et al., 2019).

Bolted Connections

Bolt are preferred for high strength steel constructions duet o easier supervision, higher capacity, and adjustability (Dewobroto, 2015). A325 bolts, common for splices and end plate joints, have minimum tensile strength Fu+830 and yield stress Fy+640 MPa (Peixoto et al., 2017). Stress strain behaviour varies with temperature as shown below.

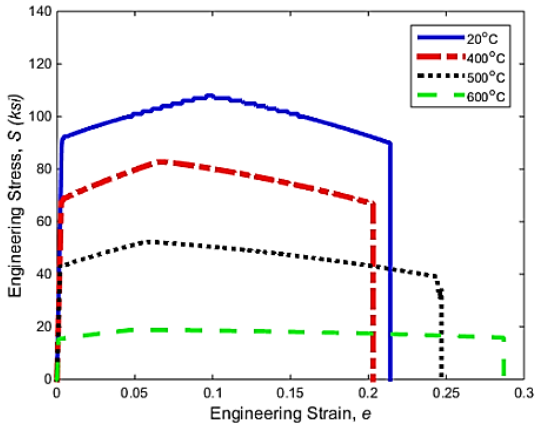

Figure 3. Stress Strain Curve A325 Bolt on Different Temp (Seif et al., 2016)

Failure modes include bolt shear, plate hole failure, bearing stress, edge shear and double shear in butt connections (Pertiwi et al., 2023). Bolt deformation under shear is illustrated.

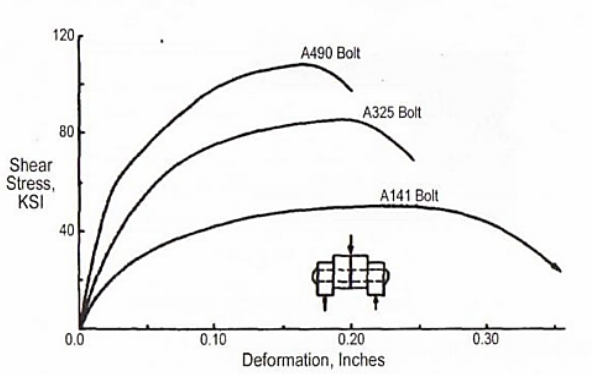

Figure 4. Graph Bolt Deformation With Shear Forces (Dewobroto, 2015).

End plate connections involve welding a plate to the member end, bolted to others for beam to column or beam to beam joints, categorizes into flush and extended types (Sumner & Murray, 2002)

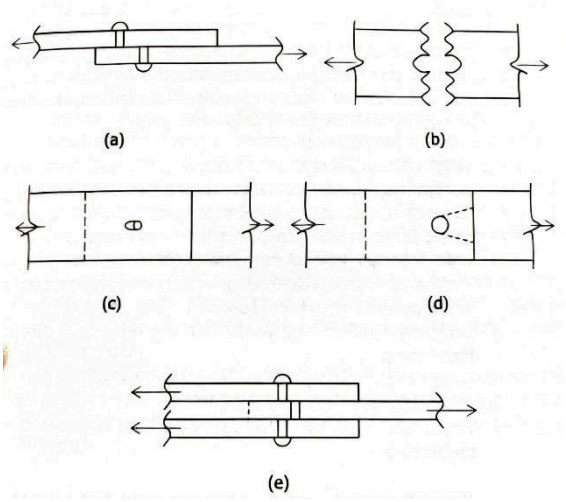

Figure 5. Type of Plate Connection Failure
(Pertiwi et al., 2023)

Block Shear Failure occurs in specific configurations, with shear along longitudinal lines and tension across transverse sections (Segui, 2012).

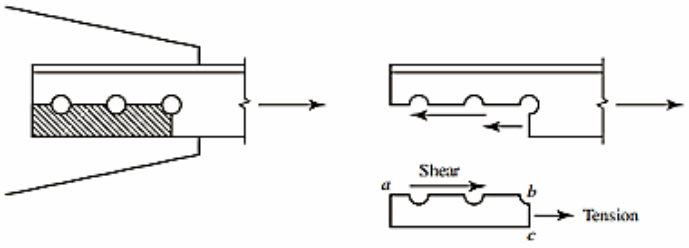

Figure 6. Block Shear Illustration on Single-Side Stress (Segui, 2012)

These mechanisms determine connection limiting strength, including fracture at net sections, yielding at gross sections, shear, bearing or tensile failures (Baehaki et al., 2019). To determine the capacity of a connection, the experimental method is the approach that most closely approximates actual conditions. However, time, cost, equipment, and human resources must be taken into consideration (Firdaus et al., 2022).

Finite Element Method (FEM)

When a structural problem involves a complex geometric shape, irregular loading, or complicated material properties, obtaining a solution through analytical calculations can be challenging. An analytical solution is a mathematical approach that can only be applied to a limited number of conditions and locations within a structural or physical system. Generally, analytical solutions require solving differential equations, which is often hindered by the complexities mentioned above regarding geometry, loading, and material properties (Logan, 2012).

The Finite Element Method (FEM) is a numerical technique used to solve problems in engineering science and mathematical physics. The scope of the issues solved includes structural analysis, heat transfer, fluid flow, mass transport, and electromagnetic potential. As the name suggests, FEM analysis is based on representing a body or structural system as a collection of

discrete elements. These elements form a network system through connections at the elements' nodal points (Nikishkov, 2004).

Finite Element Analysis (FEA) is commonly used to solve and analyze engineering-related problems such as static, dynamic, and seismic analysis (Nguyen et al., 2018). In this specific study/experiment, FEM is utilized to analyze the stress distribution occurring in the bolted connection area of the IWF steel section. The Finite Element Method (FEM) is a technique for numerically solving partial differential equations. This method is important for at least two reasons: First, FEM can solve differential equations in regions of almost any arbitrary shape. Second, the method is highly suitable for a broad class of differential equations (Wolfram, 2025). FEM is a numerical method used to solve various engineering problems, such as in this study on shear connections of steel beams and columns. Therefore, this method is employed to obtain the displacement of this steel connection structure (Pramono et al., 2018).

Non-linear static analysis is a crytical method for analyzing and understanding the detailed behaviour and eventual collapse progression of a structure. The study experimented by Prasetyo et al. (2020) use this approach using SAP2000 software to determine a buildings performance point under seismic load. This study of using advance computational analysis to evaluate structural maximum capacity justifies the use of finite element modeling to analyze similarity complex, non linear behaviour, such as the stress distributions found in the bolted steel connections.

Research Methods

This research will be structured using a literature review and a case study based on testing via the Finite Element Method (FEM). The literature review is conducted to understand the theories relevant to this study, thereby providing the foundation for developing the literature review section, the conceptual framework, determining the hypothesis, conducting the analysis, and drawing conclusions from the research. The case studies on splice plate and endplate bolted connection were analyzed to evaluate their nonlinear behavior under flexural and shear loading. In addition, a plain IWF beam without connections was included as a benchmark to provide a direct comparison with literature findings and to assess how the connections affect overall structural performance, stiffness, and load capacity relative to a uninterrupted beam.

The stages and flow of the research are carried out as follows:

1. Literature Study and Review
   a. Conducting a study and literature review from several credible sources related to the research.
   b. Sources include books, journals, scientific articles, SNI and other sources relevant to the research topic.
2. Determine Research Parameters
   a. Specifying the type of bolted connections to be analysed (Splice Plate dan End Plate)
   b. Establishing the necessary data, such as connection structure dimensions, bolt hole dimensions, and the material grades used (SS400 and A325).
3. FEA Modelling and Simulation
   a. Using *MIDAS FEA NX software to create a connection model*
   b. Perform analysis using the element method up to a non-linear approach.
4. Analysis Implementation and Interpretation
   a. Conducting analysis and simulation processes on MIDAS
   b. Analyze the results obtained such as Load-Displacement curves, stress and stiffness distribution patterns

5. Answer and Conclusion
   a. Using the data obtained from the results of the analysis to answer the problem formulation and achieve the research objectives that have been set.

For the connection design, an initial analysis of the connections will be performed using manual calculations for both splice and end-plate connection types, following established design guides and regulations.

The Test Specimen Data encompass the grade and dimensions of the IWF (Wide Flange) steel section, connection plates, and bolts. Designs follow SNI 1729 and AISC. The specifications include:

- IWF Section : 400x200x13x8x16 (Gunung Garuda)
- Section Grade : SS400 (Fy: 235 MPa, Fu: 400 MPa)
- Total Span : 10 m (9 m effective support span with pin-roller support)
- Connecting plates : 8 mm and 16 mm thick
- Bolt Grade : A325
- Bolt Dimension : M20 and M24

The model simulate a 9m effective span IWF beam under four point bending, with variations in conection possitions. Supports are pin-roller at ends, and loads are applied at 3m from each support. This setup ensures realistic flexural-shear interaction, with the connection at mid span or side span.

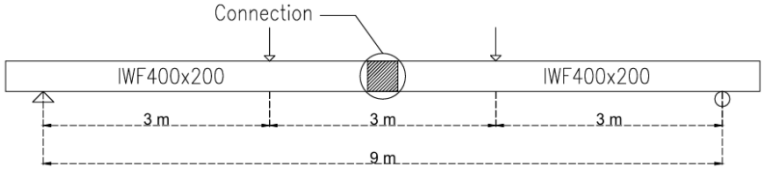

Figure 7. Illustration of Beam Model and Loading Positions

The material properties for the SS400 steel profile and plates will utilize data from previous experiments, as shown in Figure 1 The same approach is used for the A325 steel grade, following previous experiments, as shown in Figure 3.

Table 2. Steel Dimension and Grade SS400

Section	d	b	tf	tw	fy	Fu
IWF 400 x 200	400	200	13	8	245	400

Table 3. Bolt Dimension and Grade A325

Bolt		y	u
M 20	0	32	42
M 24	4	32	42

To verify the FEM model accuracy in the elastic phase, manual calculation were performed using Macaulay's Method for beam deflection under a four-point loading configuration (load P=50 kN at 3m from each support on a 9m span IWF beam). The method integrates the moment equation stepwise, yielding a maximum deflection of -27.3 mm at mid-span.

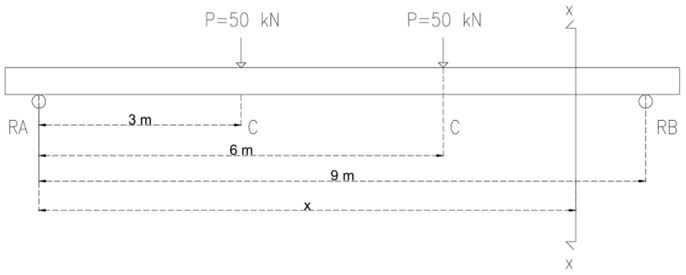

Figure 8. Manual Calculation Model Illustration

This was compared to MIDAS FEA NX results: -27.1mm confirming syncronization with <1% discrepancy. These checks ensure the model's reliability before nonlinear analysis.

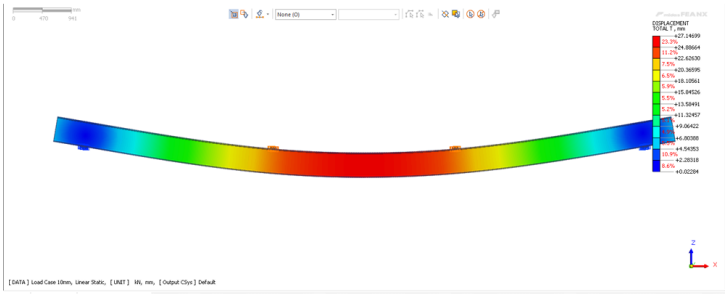

Figure 9. Analysis Result for IWF Deflection

Modeling Assumption and Limitations

This IWF profile was modeled in MIDAS FEA NX using 3D solid elements for accurate stress visualization. Key assumption include: contact modeling assumed frictionless interface between plate and beam to simulate idealized bolted connection without slip. Bolts were modeled as 1D rigid link, capturing shear and axial forces but not detailed thread deformation.. The 1D bolt assumption underestimate local stress distribution in bolts, analysis focuses on global behaviour. Non cyclic loading or fatigue was considered, and perfect fabrication was assumed.

IWF Section Model

This experiment was conducted using an IWF 400 x 200 steel section with SS400 steel grade, modelled in the MIDAS software as a 3D solid element. The loading was applied as a four-point loading with pin-roller supports. The total span of the IWF steel beam is 10m, with a span between supports measuring 9 m. For the splice connection, a 5 mm gap was introduced between the two connected sections.

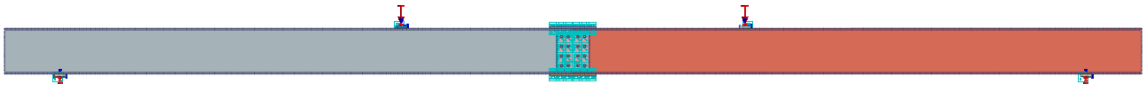

Figure 10. IWF Model With Splice Middle Connection

IWF Material Data

The main structural element used in this experiment is SS400 steel, which is commonly utilized in construction. The material data employed in the analysis refers to the material test results from previous research. The stress-strain curve for the SS400 grade steel is inputted in graphical form. This is necessary to analyze the non-linear material behavior during the connection stress analysis.

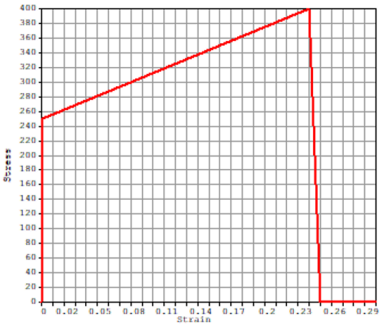

Figure 11. Stress-Strain Curve Steel SS400 on Midas FEA

Bolt Material Data

The connections in the model utilize ASTM A325 type bolts, classified as high-strength bolts. The bolt material data is presented in the following table. The bolt model is incorporated as a line element with a rigid link around the bolt hole.

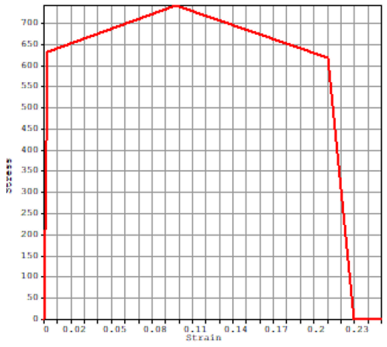

Figure 12. Stress-Strain Curve Bolt A325 on Midas FEA

Research Results and Discussion

This research aims to analyze the stress distribution in the steel section for both splice and end-plate bolted connection types. The experiment was conducted using the MIDAS FEA NX software as the primary application for obtaining the distribution and deflection results within the connections. The modeling was carried out with the steel profile element defined as Solid 3D and the bolts analyzed as rigid links. The primary outputs obtained were the stresses occurring in the profile and the connecting plates. The experiment was conducted using two connection types (splice plate and end-plate) and two connection locations (mid-span and side-span), resulting in a 2x2 design matrix of four models. Additionaly, a plain IWF beam without connection served as a benchmark comparison.

Midas FEA NX Modelling Results

The analysis modeling was performed using the MIDAS FEA NX software, which was selected for its capability in analyzing non-linear behavior and contact in detail. The modeling stages included: model creation, meshing, interface definition, boundary condition setting, and loading application.

The meshing element used in this modelling use hybrid mesher. Several boundaries were defined, specifically at the support plates and the loading plates. At the points of loading and restraint, a rigid link was implemented so that the load or boundary condition was applied at only a single node. In the model, the bolts were modeled as a 1D element with a rigid link surrounding the bolt holes for restraint. The support points were modelled as 200 mm x 100 mm plates, which were defined as solid elements, and an interface was then established to prevent relative slip between the support plate and the IWF profile.

The main result observed is the relationship between Load and Displacement at a control point located at the mid-span. The analysis was conducted with incremental loading until it reached a fully non-linear condition. The target deflection at the nodal point on the loading plate was -360 mm.

Stress Distribution Details of End Plate Connection

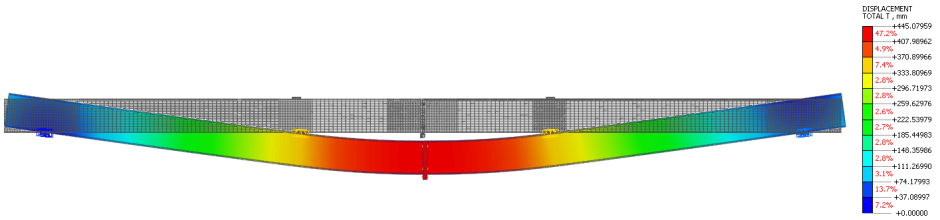

Figure 13. End Plate Middle Connection Deformation

The displacement contour reveals a critical concentration of stres sat the connection interface. The maximum displacement (indicated by red) occurs at the mid-span, where the bending is at peak, causing the end plate to undergo tension Conversly, the minimum displacement (indicated in blue) is observed at the focal point or supports, where the boundary conditions restrict movement. Mechanically, the end plate connection behave as a semi rigid interfave where the load is transfered primarity through the tension in the upper bolt row and compression at the bottom flage contact area. This distribution confirms that the end plate effectively maintains structural continuity, mimicking the behaviour of a continous beam. This phenomenon is consistent with findings in studies by Fakih et al. (2018) and Osman & Mourad (2021) who stated that end plate joints undergo significant deformation around the mid zone as the loading gradually increases until it reaches a full plastic state.

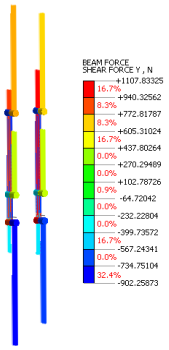

Figure 14. Shear Force Bolt Y Axis End Plate Middle Connection

The internal shear force distribution in the Y-direction across the vertical elements of the connection is illustrated in figure above. The contour reveals that the peak positive shear forces are concentrated at the beam to plate interface, where the vertical load from the beam is first transferred into the connection assembly. The maximum positive shear is recorded at +1107.835 N, while the peak negative shear reaches –902.26 N.

The distribution pattern demonstrate that the most significant shear gradient occurs at the junction zone between the beam and the end plate. Mechanically, this area acts as a zone of concentrated stress resulting from the interaction between the transverse shear load and the primary bending moment. The reduction of shear force toward the center of the beam indicates an effective transfer of forces that have been successfully distributed through the bolt group and the end plate. This phenomenon is characteristic of end-plate connections, where the shear stress

is initially localized around the bolt and the connecting plate before being dissipated into the column web and flanges.

This pattern aligns with the findings of Bahaz et al. (2018), who stated that the maximum shear force in steel joints typically occurs at the junction of beams due to the interaction between transverse loads and bending deformation. In addition, Diaz et al. (2018) also reported that increased joint stiffness will magnify the shear force gradient in the joint region, as seen in the red colour concentration in this image.

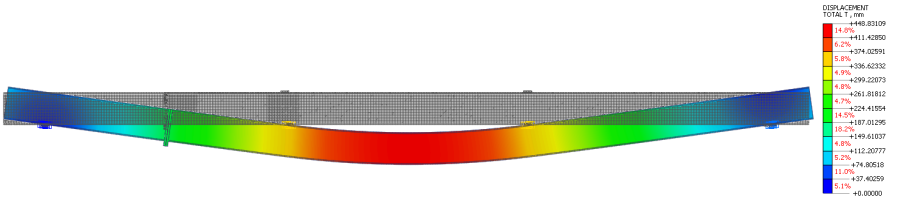

Figure 15. End Plate Side Connection Deformation

The total displacement distribution for the end plate joint shows a peak value of 448.83 mm at mid-span, aligning with the maximum bending moment in a two-support flexural system. This global deformation pattern indicates that the joint maintains sufficient rotational stiffness to allow the beam to behave as a continuous structural element. The lack of localized distortion at the interface suggests the connection remains within the elastic range, as supported by Kennedy & Hafez (2011), who noted that well-designed end-plate joints effectively shift deformation to the beam body.

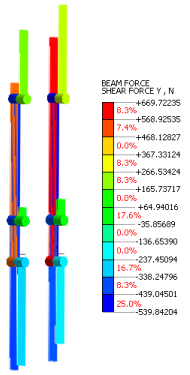

Figure 16. Shear Force Bolt Y Axis End Plate Side Connection

Regarding the internal force distribution, the Y-directional shear contours reveal a peak positive shear of +669.72 N and a peak negative (resistive) shear of –539.84 N. Mechanically, the concentration at the beam-to-plate junction represents the primary load path where the beam web transfers vertical forces to the bolt group through bearing and interface friction.

Crucially, the FEA results demonstrate that the selection of connection location is the primary determinant of the force magnitude within the bolts. Positioning the joint at mid-span subjects the bolts to maximum tensile demand due to peak flexural stress, whereas placing the connection at the side-span transitions the demand to a shear-dominant state. This distinction is vital for optimizing joint safety margins, as the mid-span location results in significantly higher stress concentrations compared to locations with lower moment-to-shear ratios.

The analysis illustrates a significant load transfer mechanism from one beam to another, dictated by the global behavior and stiffness of the connection assembly. The simulation results show a consistent load-displacement pattern across both connection types, reaching a maximum load of approximately 200 kN before entering the plastic phase. This structural response leads to

a total mid-span deflection ranging between 436 mm and 445 mm, while the side-span between 447 mm and 448 mm. Mechanically, the observed stress distribution is concentrated at the beam connection. The concentration of internal stress signifies the transition of forces through the bolt groups and connecting plates, ensuring that the load is effectively channeled to the supporting structure. These results align with the findings of Bahaz et al. (2018) and Diaz et al. (2018), confirming that the joint's efficiency is a function of its ability to redistribute stresses while maintaining structural stability.

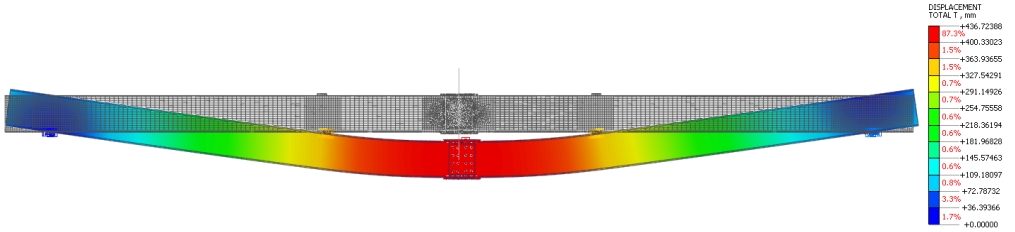

Figure 17. Splice Middle Connection Deformation

The total displacement distribution for the mid-span splice connection reaches a peak of 436.72 mm at the joint center. This global flexural response demonstrates that the splice plate effectively maintains structural continuity, allowing for efficient load transfer between the beam segments. Consistent with Tao et al. (2017), the deformation remains dominant in the beam body, indicating that the connection stiffness is sufficient to prevent premature localized plastic failure at the joint interface under the current loading stage.

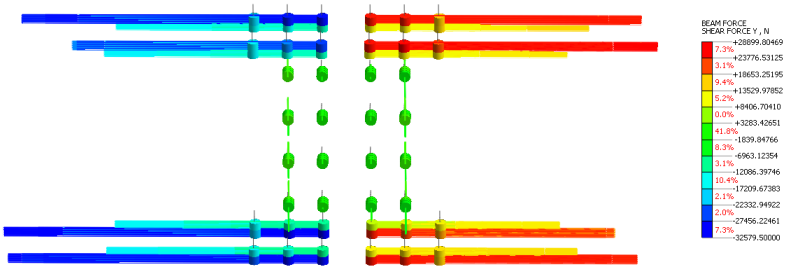

Figure 18. Shear Force Bolt Y Axis Splice Middle Connection

The Y-directional shear force distribution reveals a peak positive shear of +28,999.80 N and a peak negative shear of –32,579.50 N. Mechanically, the concentration of force is most pronounced in the outermost bolt rows. This distribution highlights an important aspect of engineering judgment: the outer bolts act as the primary resistance against the combined effects of transverse shear and the rotational torque induced by the bending moment.

These results confirm that the selection of the mid-span location significantly dictates the force magnitude on the bolts. Because the mid-span is a zone of peak bending moment, the outer bolts in this splice configuration must resist a high-magnitude combined load (shear and torque), as noted by Luo et al. (2020) and Merad et al. (2020). This contrasts with side-span placements where lower moments would result in a more uniform shear distribution across the bolt group, thereby increasing the connection's safety margin

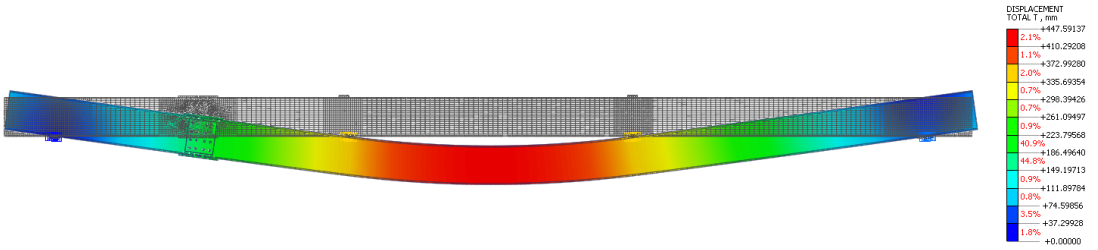

Figure 19. Splice Side Connection

The total **displacement** distribution for the splice joint with increased connection length shows a peak of 447.59 mm at mid-span. Mechanically, the extended joint length facilitates a more gradual transition of flexural stress across the connection interface. This geometric optimization results in a redistribution of global deformation, effectively reducing localized strain. As established by Song et al. (2024), increasing the joint length enhances the flexural stiffness and minimizes relative rotation between the connected beam segments, allowing the assembly to behave more like a monolithic member.

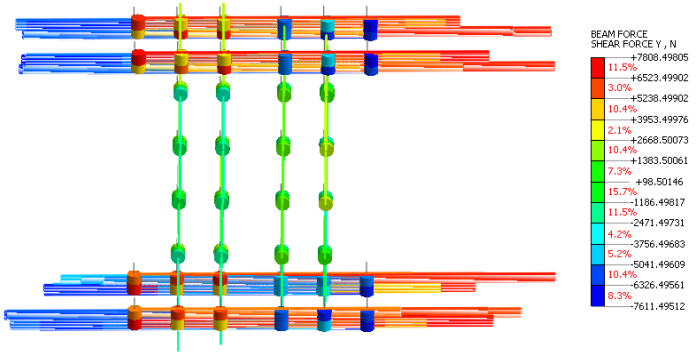

Figure 20. Shear Force Bolt Y Axis Splice Side Connection

The Y-directional shear force distribution records a peak positive shear of +7,808.50 N and a peak negative shear of –7,611.50 N. Unlike shorter connections, the extended splice configuration demonstrates a more uniform shear gradient across the bolt group. This distribution reveals a key piece of engineering judgment: by increasing the contact area and the number of active bolts, the bending moment is dissipated over a larger group, significantly lowering the force demand on individual bolts.

These results emphasize that the selection of both location and joint geometry dictates the magnitude of forces occurring on the bolts. In this mid-span configuration, the extended length mitigates the high-stress concentrations typically seen in the outer bolt rows of shorter splice joints. This increased efficiency in force transfer, as corroborated by Tong et al. (2018), directly improves the total shear capacity and safety margin of the joint by decreasing local stress concentrations at the outermost fasteners.

Analysis Results of Load and Displacement in Steel Profile and Bolts

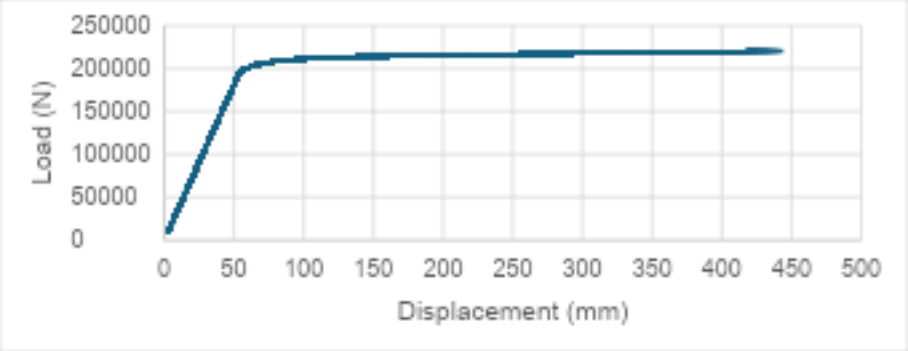

Figure 21. Load vs. Displacement, End Plate Middle Connection

The graph in Figure 18 shows the relationship between *load* and *displacement* at the end *plate middle connection*. It can be seen that the graph undergoes a sharp increase in load to about **210 kN** in the early stages of loading (about 0–80 mm), which indicates an elastic response of the joint. After reaching the peak load, the curve shows a horizontal inclination, indicating that the structure has entered the plastic stage, where the increase in additional load no longer results in significant deformation.

This pattern indicates that the end plate joints have a high initial stiffness with the ability to efficiently withstand bending loads before reaching the melting point. The response reflects the concentrated stress distribution around the bolt and the contact area between the end plate and the beam flange. These results are in line with research by Tao et al. (2017) who explained that end plate joints exhibit semi-rigid behavior with a decrease in stiffness after the initial elastic phase due to the formation of local deformations around bolts and plates.

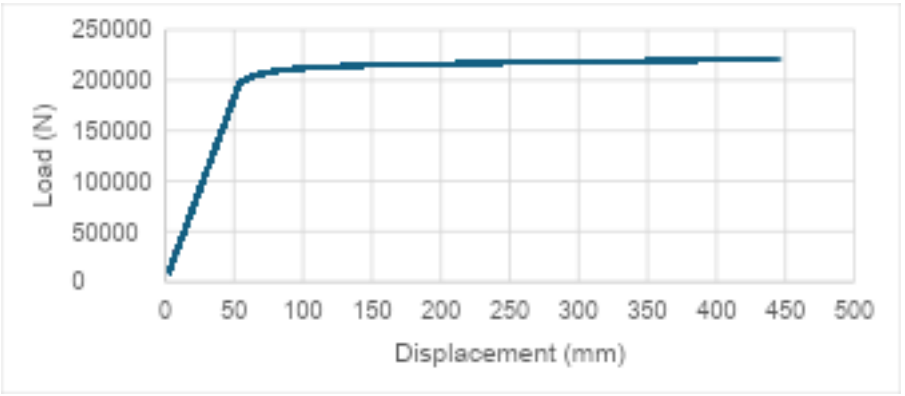

Figure 22. Graph of Load VS Displacement, End Plate Side Connection

Figure 19 shows a graph of the load and displacement relationships for the end *plate side connections*. The graph pattern is similar to that of the middle joint, where the load increases sharply to about 205 kN, then tends to stabilize once the displacement reaches about 100 mm. This suggests that plastic deformation behavior also occurs after crossing the elastic boundary.

The side joints show a slight decrease in rigidity compared to the middle joint, which may be due to the influence of the base or the difference in the distribution of flexural moments along the beam. Greater voltage distribution on one side of the joint may cause local rotation, reducing the total energy absorption capacity. These findings are consistent with the numerical results of Gomes et al. (2018) who suggested that the position of the connection against the main bending axis affects the rotational capacity and redistribution of forces between bolts.

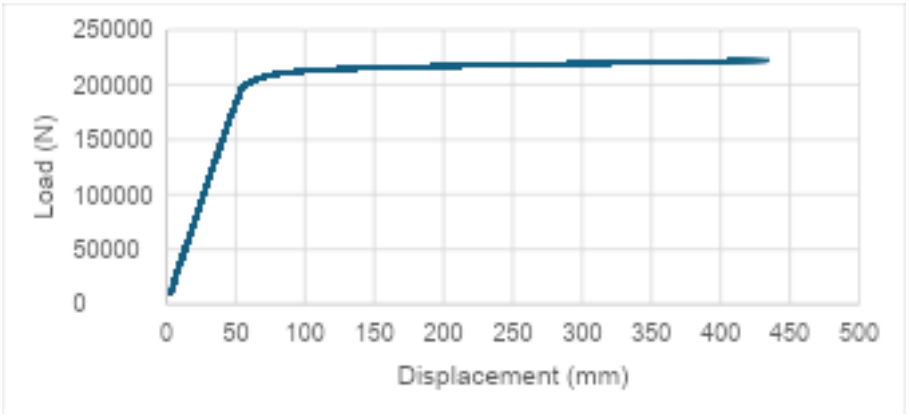

Figure 23. Graph of Load VS Displacement, Splice Middle Connection

Figure 20 shows the results of the analysis of the load and displacement relationship in the middle connection of the *splice* type. The curve pattern shows a rapid load increase of up to about 210 kN at the beginning of loading, followed by a flat section that signifies non-linear behavior once the elastic limit is reached. This shows that the *splice* joint has a high initial stiffness and is able to efficiently transfer axial and bending forces between beam segments.

This behavior also shows that the highest tension is concentrated on the fastening bolts in the joint area, while the beam body undergoes greater global deformation. This response is in line with the results of research by Fakih et al. (2018) who reported that *the splice* joints showed a dominant deformation in the beam body, while the bolts experienced a progressive increase in shear force until the melting condition of the bolts or plates was achieved.

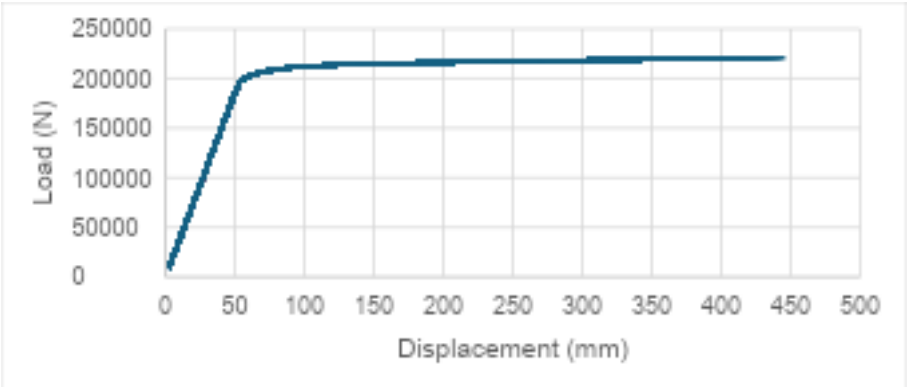

Figure 24. Graph of Load VS Displacement, Splice Side Connection

The graph in Figure 21 illustrates the displacement-load relationship for the *splice* joints located on the sides of the beam. The curve has a similar tendency to the middle joint, with a maximum load of about 205 kN, but shows a slight shift at the point of plastic deformation. This indicates that the side joints undergo faster force redistribution due to the difference in structural rigidity between the beam segments and the joints.

Side joints exhibit a relatively greater deformation ability, with a slight decrease in initial stiffness, compared to middle joints, demonstrating good ductile connection characteristics that resist deformation without a significant loss of load capacity. This pattern reinforces the finding of Tork-Ladani et al. (2019) that *splice* joints placed in areas with high voltage gradients exhibit greater rotational deformation, but still retain load capacity until the complete plastic stage.

Table 5. Max Displacement and Load on Connection

Connection	Connection Position	Max Displacement (mm)	Max Load (kN)
Plain IWF	-	456	222.0
End Plate	Middle Span	445	220.5
End Plate	Side Span	448	220.9
Splice	Middle Span	436.7	222.2
Splice	Side Span	447	221.1

All four models exhibited a similar pattern in the Load–Displacement curve, an initial linear load increase during the early increment stages, indicating an elastic response. This was then followed by a reduction in stiffness until a plastic region formed, where the load remained relatively constant despite increasing displacement. This observation indicates that all models exhibited stable plastic behaviour without any significant signs of strength degradation.

Among all connection types, the splice middle connection showed the smallest maximum displacement (He et al., 2020; Zhang, et al. 2025), suggesting that the splice connection type at the mid-span is relatively stiffer compared to the other configurations. However, the overall difference in displacement among the models was not significant. Therefore, it can be concluded that the difference in connection position or connection type does not significantly affect the global stiffness of the IWF section structure during the non-linear stage.

The load-displacement curves indicate that all four connections were able to withstand a load of approximately 200 kN before reaching a significant state of plastic deformation. After passing this stage, the graph began to flatten, signifying that the profile had reached its yield capacity. The absence of capacity reduction after the maximum point indicates that the structure remained stable and had not experienced failure even after exceeding the allowable displacement limit of L/240.

Conclusion

The nonlinear finite element analysis using MIDAS FEA NX demonstrated stable load-displacement behavior across the four models, with maximum loads of 220.5–222.2 kN and maximum displacements of 436.7–448 mm. All configurations exhibited an initial elastic phase up to 200–210 kN followed by ductile plastic transition with no significant strength degradation. The splice mid-span model provided the highest stiffness , while the end-plate mid-span model most closely matched the plain IWF benchmark. Among the models, the end-plate connection at mid-span is the most efficient, offering near-monolithic performance with fewer bolts and reduced fabrication needs. End-plate connections generally mimic plain beam behavior better, while splice provides superior stiffness at mid-span and side-span positions improve bolt force uniformity for both types. Model reliability is supported by analytical validation by Macaulay's Method deflection matching FEM within <1% and alignment with literature benchmarks. Future work should include fatigue testing, varied configurations, and experimental validation to enhance practical application.

References

Abdi, M., Bachtiar, G., & Daryati. (2017). Penggunaan Multimedia Interaktif berbasis Computer Assisted Instruction (CAI) pada Topik Pembahasan Baja sebagai Bahan Bangunan. *Jurnal Pendidikan Teknik Sipil, 6*(2), 1–9.

ACI Committee 318. (2014). *Building Code Requirements for Structural Concrete (ACI 318M-14) and Commentary (ACI 318RM-14).* In American Concrete Institute.

Akhmad, A. (2019). Studi Eksperimental Dan Analisis Kapasitas Sambungan Baja Akibat Eksentrisitas Pelat Sambung. *Jurnal Ilmiah Teknik Sipil*.

Alzahri, S., & Albimanzura , S. R. (2022). Perilaku Sambungan Baut Flush End-Plate Balok Kolom Menggunakan Ansys Work Bench. *Teknika jurnal Teknik*.

Anugrah, P. (2023). *Desain Struktur Gedung Beton Bertulang Dengan Etabs Versi 18.1.1*. Malang: UB Press.

Anwar, K. M., & Pradnya, P. S. (2022). Analisis Kekuatan Sambungan Baut Mutu Tinggi Tipe Tumpu Pada Struktur Baja Jembatan. *Jurnal Pensil: Pendidikan Teknik Sipil*, 1–10.

Arifi, E., & Setyowulan, D. (2021). *Perencanaan Struktur Baja (Berdasarkan SNI 1729:2020)*. Malang: UB Press.

Artha, S. O. (2020, Februari). Studi Analisis Perilaku Sambungan Kaku (Rigid Connection) Balok – Kolom Baja Tipe Extended End Plate dengan Metode Elemen Hingga. *Jurnal Aplikasi Teknik Sipil, Volume 18*(Nomor 1).

ASTM, A.-1. (2014). *Standard Specification for Structural Bolts, Steel, Heat Treated 120/105 ksi Minimum Tensile Strength*. ASTM International.

Baehaki, Aminullah, A., & Siswosukarto, S. (2019). Studi Eksperimental dan Analisis Kapasitas Sambungan Baja Akibat Eksentrisitas Pelat Sambung. *Jurnal Ilmiah Teknik Sipil: A Scientific Journal of Civil Engineering*, *23*(2), 52–60. https://doi.org/https://ocs.unud.ac.id/index.php/jits/article/view/53267

Bahaz, A., Amara, S., Jaspart, J. P., & Demonceau, J. F. (2018). Analysis of the Behaviour of Semi Rigid Steel End Plate Connections. *MATEC Web of Conferences*. https://doi.org/https://doi.org/10.1051/matecconf/201714902058

Bilina, T., Dwi, H. B., & Ronny, P. (2017, Juli). Perilaku Sambungan Baut Flush End-Plate Balok Kolom Baja Pada Kondisi Batas. *Jurnal Sipil Statik, Vol. 5*(No. 5), 237-247.

Dermawan, Z. (2023). *Struktur Baja Pemahaman dan Contoh Penyelesaian*. Purwokerto: Amerta Media.

Dewobroto, W. (2015). *Struktur Baja Perilaku, Analisis & Desain - AISC 2010*. Jakarta: Luminsa Press.

Diaz, C., Victoria, M., Querin, O. M., & Marti, P. (2018). FE Model of Three-Dimensional Steel Beam-to-Column Bolted Extended End-Plate Joint. *International Journal of Steel Structures, 18*(3), 843–867. https://doi.org/https://doi.org/10.1007/s13296-018-0033-y

Fakih, K. A., Chin, S. C., & Doh, S. I. (2018). Behavior of Extended End-Plate Steel Beam to Column Connections. *The Open Civil Engineering Journal, 12*(1), 250–262. https://doi.org/https://doi.org/10.2174/1874149501812010250

Firdaus, M., Setiobudi, A., Alzahri, S., & Albimanzura, R. M. (2022). Perilaku Sambungan Baut Flush End-Plate Balok Kolom Menggunakan Ansys Work Bench. *TEKNIKA: Jurnal Teknik, 9*(1). https://doi.org/https://www.teknika-ftiba.info/teknika/index.php/1234/article/view/220

Gerard, T. J. (2017, November). Pengaruh Variasi Panjang Pelat Pengaku Flush End Plate Terhadap Kekuatan Sambungan Balok Ke Balok. *Jurnal Sipil Statik, Vol.5*(No.9), 571-578.

Gomes, V., Silva, A. T., de Lima, L. R., & Vellasco, P. C. (2018). Numerical investigation of semi-rigid connection ultimate capacity. *Revista Escola de Minas*, 505–512. https://doi.org/https://doi.org/10.1590/0370-44672018710031

Hai, V. G., Minh, H. T., & Toan, D. N. (2020). A Study On Experiment and Simulation To Predict The Spring Back Of SS-400 Steel In Large Radius Of V-Bending Process. *School of Mechanical Engineering*.

Hai, V. G., Minh, N. T., & Toan, N. D. (2019). Mechanical Properties Of Steel SS400 Steel Plate at Elevated Temperatures. *Applied Mechanic and Materials*, 51-57.

Hai, V., Min, N. T., & Nguyen, D. T. (2020). A study on experiment and simulation to predict the spring-back of SS400 steel sheet in large radius of V-bending process. *Materials Research Express, 7*(1). https://doi.org/https://doi.org/10.1088/2053-1591/ab67f5

Hanafie, J., & Surjokusumo, S. (2020). Studi Perbandingan Perilaku Struktur Rangka Baja dengan Sambungan Baut dan Las. *urnal Pensil: Pendidikan Teknik Sipil*, 35–46.

Haris, P. (2018). Analisis Sambungan Baut Pada Titik Buhul Jembatan Rangka Baja Menggunakan Metode Elemen Hingga. https://www.academia.edu/87298481/Analisis_Sambungan_Baut_Pada_Titik_Buhul_Jembatan_Rangka_Baja_Menggunakan_Metode_Elemen_Hingga.

He, R., Zhang, Z., & Li, J. (2020). Experimental Study on Bolt-Spliced Prefabricated Steel Frame Beams. *Advances in Civil Engineering*. https://doi.org/https://doi.org/10.1155/2020/6191475

Kennedy, D., & Hafez, M. (2011). A study of end plate connections for steel beams. *Canadian Journal of Civil Engineering, 11*, 139–149. https://doi.org/ https://doi.org/10.1139/l84-026

Lesmana. (2021). *Handbook Analisa Desain Struktur Baja Berdasarkan SNI*. Yogyakarta: PT.Nas Media Indonesia.

Linggasari, D., Sutandi, A., & Kushartomo, W. (2019). Pengaruh Tepung Marmer Terhadap Sifat Mekanik Reactive Powder Concrete. Jurnal Muara Sains. *Teknologi, Kedokteran Dan Ilmu Kesehatan, 2*(2). https://doi.org/https://doi.org/10.24912/jmstkik.v2i2.3013

Logan, D. L. (2012). *A First Course In The Finite Element Method. Stamford:*.

Luo, L., Du, M., Yuan, J., Shi, J., Yu, S., & Zhang, Y. (2020). Parametric analysis and stiffness investigation of extended end-plate connection. *Materials, 13*(22), 1–30. https://doi.org/https://doi.org/10.3390/ma13225133

Merad, B., Boumechra, N., Bouchair, A., & Missoum, A. (2020). Modeling of bolted endplate beam-to-column joints with various stiffeners. *Journal of Constructional Steel Research*. https://doi.org/https://doi.org/https://doi.org/10.1016/j.jcsr.2020.105963

Mina, S., Main, J., Weigand, J., Sadek, F., Choe, L., Zhang, C., Gross, J., Lueeke, W., & McColskey, D. (2016). *Temperature-Dependent Material Modeling for Structural Steels: Formulation and Application*. National Institute of Standards and Technology.

Nguyen , N. V., Kim, J. J., & Kim, S. E. (2018). Methodology to Extract Constitutive Equation at a Strain Rate Level From Indentation Curves. *International Journal of Mechanical Sciences*. https://doi.org/https://doi.org/10.1016/j.ijmecsci.2018.12.023

Nikishkov, G. P. (2004). Introduction to the Finite Element Method. *Indian Institute of Technology Guwahati*. https://doi.org/https://doi.org/10.7142/igakutoshokan.55.211

Oktaviandy, N. R., Kardiman, & Hanafi, R. (2023). Effect Of Preheat Temperature Variation With Cooling Media On Mechanical Properties In Welding SS400 Steel. *Journal Ilmiah Teknik Mesin, 17*(2), 130-142. https://doi.org/ 10.24853/sintek.17.2.130-142

Osman, A. A., & Mourad, S. A. (2021). Performance of extended end-plate bolted connections

subjected to static and blast-like loads. *Journal of Engineering and Applied Science, 68*(1), 1–25. https://doi.org/https://doi.org/10.1186/s44147-021-00001-3

Peixoto, M. R., Seif, M. S., & Vieira Jr, L. (2017). Double-Shear Tests of High-Strength Structural Bolts at Elevated Temperatures. *Fire Safety Journal.*

Pertiwi, D., Susanti, E., & Propika, J. (2023). Struktur Baja SNI 1729-2020 Perilaku, Analisis, Dan Desain Struktur Baja. Surabaya: Lakeisha.

Pramono, H. S., Sutrisno, W., & Yasin, I. (2018). Analisis Sambungan Baut Pada Titik Buhul Jembatan Rangka Baja Menggunakan Metode Elemen Hingga. *RENOVASI: Rekayasa Dan Inovasi Teknik Sipil, 3*(2), 52–63.

Prasetyo, H., Kurniati, D., & Prihadi, B. K. (2020). Evaluasi Kinerja Struktur Bangunan Menggunakan Pushover Analysis Dengan Metode Atc-40 Dan Fema 356. *Jurnal PenSil, 9*(1), 40–46. https://doi.org/ https://doi.org/10.21009/jpensil.v9i1.14021

Segui, W. T. (2012). *Steel Design.* Cengage Learning. https://books.google.co.id/books?id=TXIVzgEACAAJ

Seif, M., Choe, L., Zhang, C., Gross, J., & Luecke, W. (2016). Temperature-Dependent Material Modeling for Structural Steels: Formulation and Application. *National Institute of Standards and Technology*. https://doi.org/http://dx.doi.org/10.6028/NIST.TN.1907

Song, Y., Lin, X. M., Yam, M. C., Ke, K., & Wang, J. (2024). Behaviour and design of duplex stainless steel bolted connections failing in block shear. *Engineering Structures*. https://doi.org/https://doi.org/10.1016/j.engstruct.2024.117442

Sumner, E., & Murray, T. (2002). Behavior of Extended End-Plate Moment Connections Subject to Cyclic Loading. *Journal of Structural Engineering-Asce - J STRUCT ENG-ASCE*, 128. https://doi.org/https://doi.org/10.1061/(ASCE)0733-9445(2002)128:4(501)

Tao, Z., Li, W., Shi, B. L., & Han, L. H. (2017). Behaviour of bolted end plate connection to concrete-filled steel columns. *Journal of Constructional Steel Research, 134*, 194-208.

Tayu, B., Handoyo, B. D., & Pandaleke, R. (2017). Perilaku Sambungan Baut Flush End-Plate Balok Kolom Baja pada Kondisi Batas. *Jurnal Sipil Statik, 5*(5), 237–247.

Tong, L., Mou, X., Zhou, F., Gong, J., Huan, Y., & Wang, X. (2018). Flexural Behavior of Bolt-Spliced Steel Beams. *Tongji Daxue Xuebao/Journal of Tongji University, 46*, 1175–1181. https://doi.org/https://doi.org/10.11908/j.issn.0253-374x.2018.09.003

Tork-Ladani, F., Chase, J. G., & Macrae, G. A. (2019). Bending Stiffness and Strength Performance of Different Column Splice Connections. 1–12.

Vuong, G., Minh, N., & Nguyen, D. T. (2019). Mechanical Properties of SS400 Steel Plate at Elevated Temperatures. *Applied Mechanics and Materials, 889*, 51–57. https://doi.org/https://doi.org/10.4028/www.scientific.net/AMM.889.51

Wolfram. (2025). *Solving Partial Differential Equations with Finite Elements.* https://reference.wolfram.com/language/FEMDocumentation/tutorial/SolvingPDEwithFEM.html#2013991835

Yamada, S., & Jiao, Y. (2016). A Concise Hysteretic Model of Structural Steel Considering the Bauschinger Effect. *International Journal Of Steel Structures.*

Zhang, X., Lv, J., Fan, D., Feng, S., & Yu, S. (2025). Optimisation and Mechanical Behaviour Analysis of Splice Joints in Prefabricated H-Shaped Steel Beams1–25. 1–25.